KEK Internal 2000-10
November 2000
R

Lecture Note on Photon interactions and Cross Sections

H. Hirayama

Lecture Note on Photon Interactions and Cross Sections

Hideo Hirayama

KEK, High Energy Accelerator Research Organization,
1-1, Oho, Tsukuba, Ibaraki, 305-0801 Japan

Abstract

This is the lecture note used at the "Tutorials for Electron/Gamma Monte Carlo: building blocks and applications" as part of the International Conference on the Monte Carlo 2000, Advanced Monte Carlo on Radiation Physics, Particle Transport Simulation and Applications (Monte Carlo 2000) held at Lisbon Portugal, 23-26 October, 2000.

1 Introduction

This lecture contains descriptions of the individual atomic cross sections of photons for scattering, absorption, and pair production that are necessary for photon transport calculations, together with related cross section data. Many parts on this lecture are based on the series of works by J. H. Hubbell[1, 2, 3, 4, 5, 6] in this field.

2 Classification of Interaction

The interaction of photons with matter may be classified according to:

1. The kind of target, e.g., electrons, atoms, or nuclei, with which the photons interact, and
2. The type of event, e.g., scattering, absorption, pair production, *etc.*, which takes place.

Possible interactions are summarized in Table 1.[7] As an example, the cross sections of a photon with Cu is shown in Fig. 1[8]. It is apparent from Fig. 1 that for the attenuation of photons the most important interactions are:

1. The photoelectric effect, σ_{pe},
2. Compton scattering, σ_C, and
3. Electron-positron pair production, $(\sigma_{pair} + \sigma_{trip})$.

Rayleigh scattering, σ_R, is usually of minor importance for the broad beam conditions typically found in shielding, but must be known for the interaction of attenuation coefficient data.

The photonuclear effect, $\sigma_{ph.n}$, is mostly restricted to the region of the giant resonance around 10 to 30 MeV where, at the resonance peak, it may amount to as much as 10 percent of the total "electronic" cross section.

Elastic nuclear scattering, inelastic nuclear scattering and Delbrück scattering are negligible processes in photon interactions. Elastic nuclear scattering is regard as a nuclear analog to very low energy Compton scattering by an electron. In this process, a photon interacts with a nucleon in such a manner that is a photon re-emitted with the same energy.

During inelastic nuclear scattering, the nucleus is raised to an excited level by absorbing a photon. The excited nucleus subsequently de-excites by emitting a photon of equal or lower energy.

The phenomenon of photon scattering by the Coulomb field of a nucleus is called Delbrück scattering (also called nuclear potential scattering). It can be thought of as virtual pair production in the field of the nucleus – that is, pair production followed by annihilation of the created pair.

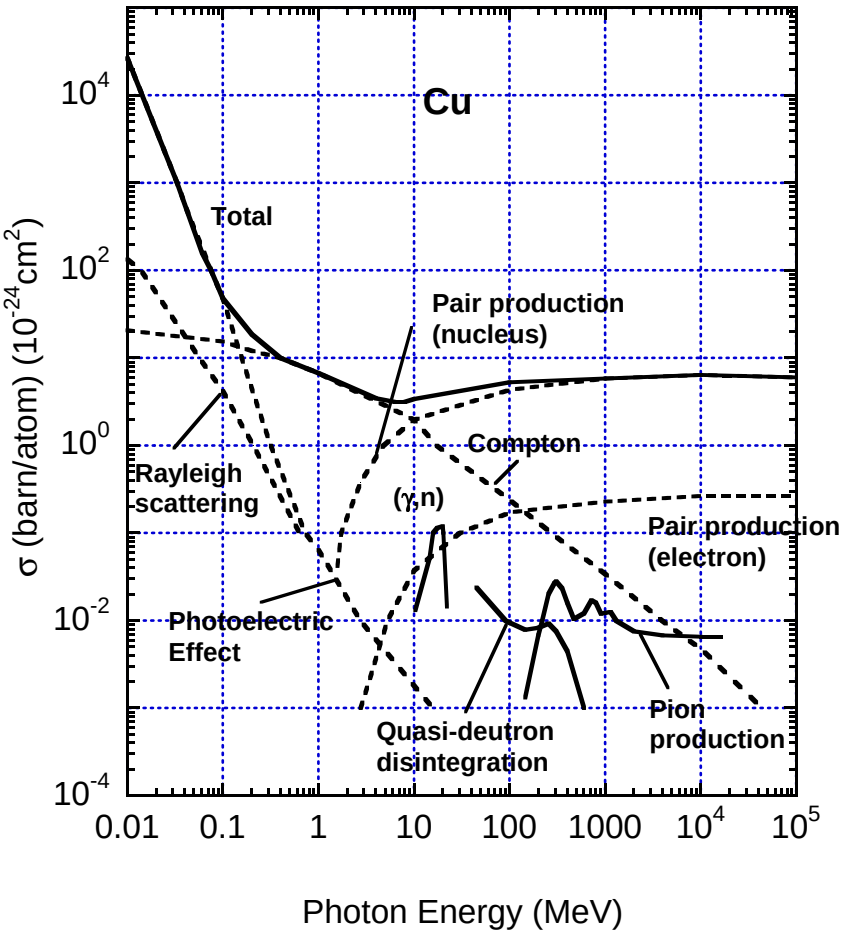

Figure 1: Cross section of Cu for photons between 10 keV and 100 GeV.[8].

Table 1. Classification of elementary photon interactions.

Type of interaction / Interaction with:	Absorption	Scattering	
		Elastic (Coherent)	Inelastic (Incoherent)
Atomic electrons	**Photoelectric effect** $\sigma_{pe} \begin{cases} \sim Z^4 (L.E.) \\ \sim Z^5 (H.E.) \end{cases}$	Rayleigh scattering $\sigma_R \sim Z^2$ $(L.E.)$	**Compton scattering** $\sigma_C \sim Z$
Nucleus	Photonuclear reactions $(\gamma,n),(\gamma,p)$, photofission, etc. $\sigma_{ph.n.} \sim Z$ $(h\nu \geq 10\text{MeV})$	Elastic nuclear scattering $(\gamma,\gamma) \sim Z^2$	Inelastic nuclear scattering (γ,γ')
Electric field surrounding charged particles	**Electron-positron pair production in field of nucleus,** $\sigma_{pair} \sim Z^2$ $(h\nu \geq 1.02\textbf{MeV})$	Delbrück scattering	
	Electron-positron pair production in electron field, $\sigma_{trip} \sim Z^2$ $(h\nu \geq 2.04\textbf{MeV})$		
	Nucleon-antinucleon pair production $(h\nu \geq 3$ GeV)		
Mesons	Photomeson production, $(h\nu \geq 150$ MeV)	Modified (γ,γ)	

3 Photoelectric Effect

Studies related to the photoelectric effect are reviewed historically by Hubbell in NSRDS-NBS 29[1].

In the atomic photoeffect, a photon disappears and an electron is ejected from an atom. The electron carries away all of the energy of the absorbed photon, minus the energy binding the electron to the atom. The K-shell electrons are the most tightly bound, and are the most important contributions to the atomic photoeffect cross-section in most cases. However, if the photon energy drops below the binding energy of a given shell, an electron from that shell cannot be ejected. Hence, particularly for medium- and high-Z elements, a plot of σ_{pe} versus the photon energy exhibits the characteristic sawtooth absorption edges, since the binding energy of each electron subshell is attained and this process is permitted to occur. These feature can be seen well in Fig. 2, which shows the total photoelectric cross section, σ_{pe}, for Ag together with subshell ones[9].

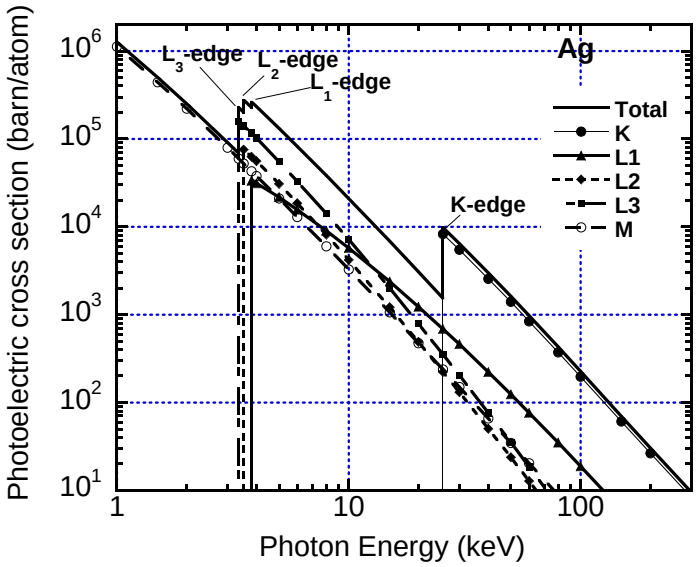

Figure 2: Total and partial atomic photoeffect of Ag.[9].

The order of magnitude of the photoelectric atomic-absorption cross section is

$$\sigma_{pe} \begin{cases} \sim Z^4/(h\nu)^3 & \text{low energy} \\ \sim Z^5/h\nu & \text{high energy.} \end{cases} \tag{1}$$

Dramatic resonance structures of the order of 10% just above the absorption edges are well known and can be easily observed with high-resolution spectrometers. Owing to their dependence on the temperature, chemical binding and other variable atomic environments, this extended X-ray absorption fine structure (EXAFS) is not included in the photon transport calculation. However, EXAFS can be a major analytical tool in X-ray diffraction spectrometry.

3.1 Relaxation processes after the photoelectric effect

A vacancy created by the ejection of an electron from an inner shells is filled by an outer electron falling into it (de-excitation); this process may be accompanied by one of the following modes:

1. A fluorescence X-ray is emitted from the atom, with a photon energy equal to the difference between the vacancy-site inner-shell energy level and energy level of the particular outer shell which happens to supply the electron to fill the vacancy (fluorescence yield, ω, is the fraction of fluorescence X-ray emission).

2. The excess energy ejects an outer-shell electron from the atom. This electron is known as an Auger electron (Auger yield, a, is the fraction of Auger emission).

3. A vacancy is filled by an electron in a higher subshell, like from the L_2 subshell to the L_1 subshell. This process is called Coster-Kronig. As a result, a new vacancy is created, in which is filled by one of the modes (Coster-Kronig yield, f, is the fraction of Coster-Kronig).

The sum of fluorescence yield, ω, Auger yield, a, and Coster-Kronig yield, f, is unity:

$$\omega + a + f = 1 \tag{2}$$

Experimental and theoretical fluorescence-yield information have been reviewed by Fink *et al.*[10], Bambynek *et al.*[11], Krause[12] and Hubbell[2].

The yields of fluorescence, Auger electrons and Coster-Kronig after the K-, L_1-, L_2- or L_3-photoelectric effect[13] are shown in Fig. 3.

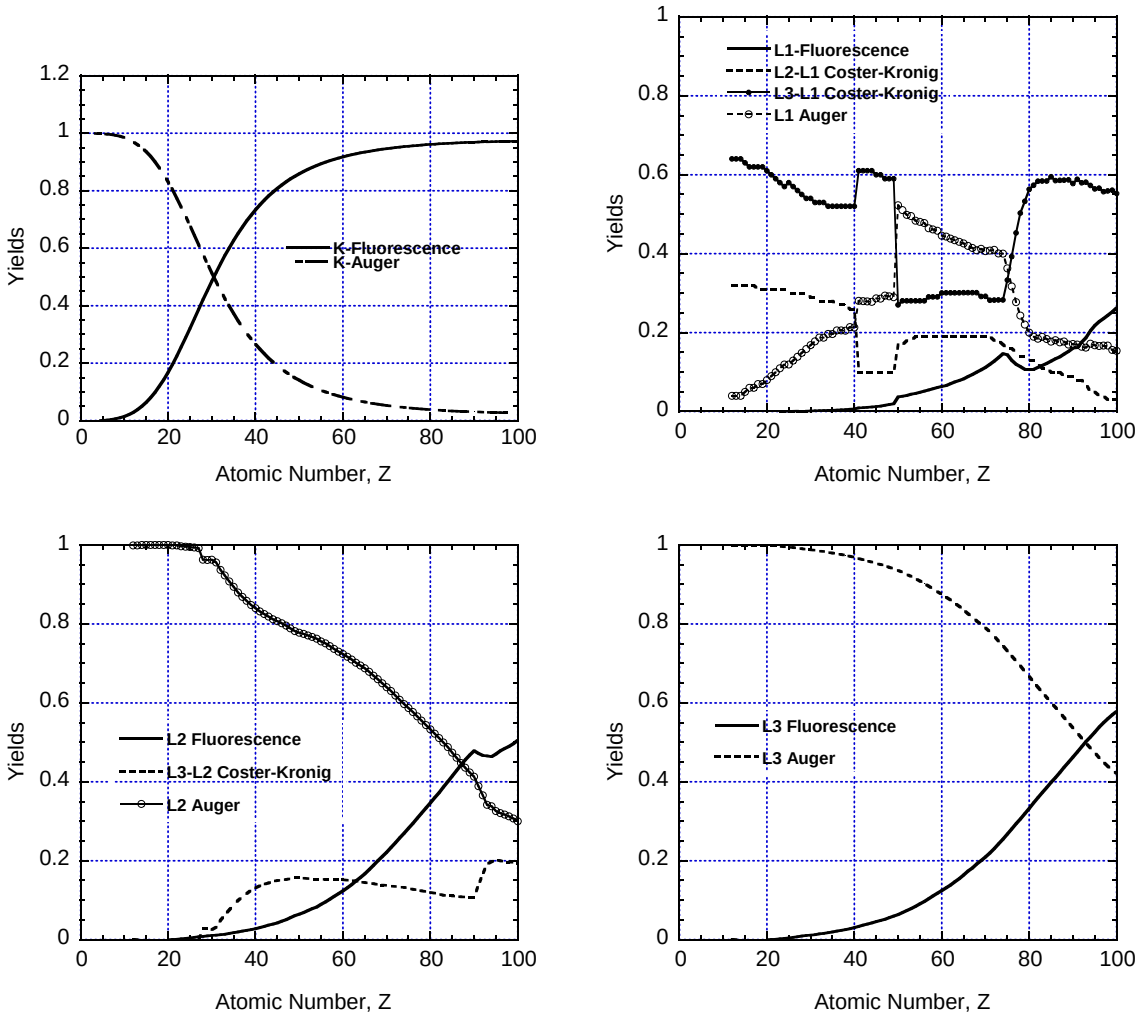

Figure 3: Yields of fluorescence, Auger electrons and Coster-Kronig after the K-, L_1-, L_2- or L_3-photoelectric effect[13].

The fluorescence X-ray intensities are important for low energy photon transport. Scofield published K and L fluorescence X-ray intensities calculated with the relativistic Hatree-Slater theory for elements with Z=5 to 104[14]. His data are cited in a Table of Isotopes Eighth Edition[13], but are slightly different with the experimental results, as presented by Salem *et al*[15].

4 Scattering

4.1 Compton scattering, Klein-Nishina Formula

In Compton scattering, a photon collides with an electron, loses some of its energy and is deflected from its original direction of travel (Fig. 4). The basic theory of this effect, assuming the electron to be initially free and at rest, is that of Klein and Nishina[16].

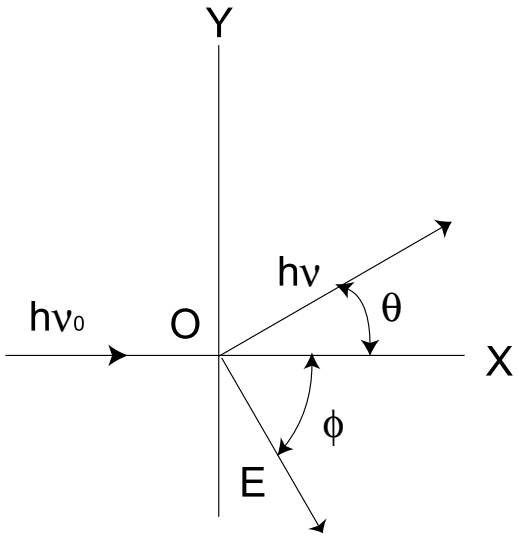

Figure 4: Compton scattering with a free electron at rest.

The relation between photon deflection and energy loss for Compton scattering is determined from the conservation of momentum and energy between the photon and the recoiling electron. This relation can be expressed as:

$$h\nu = \frac{h\nu_0}{1 + \left(\frac{h\nu_0}{m_e c^2}\right)(1 - \cos\theta)}, \tag{3}$$

$$E = h\nu_0 - h\nu = m_e c^2 \frac{2(h\nu_0)^2 \cos^2\phi}{(h\nu_0 + m_e c^2)^2 - (h\nu_0)^2 \cos^2\phi}, \tag{4}$$

$$\tan\phi = \frac{1}{1 + \left(\frac{h\nu_0}{m_e c^2}\right)} \cot\frac{\theta}{2}, \tag{5}$$

where $h\nu_0$ is the energy of incident photon, $h\nu$ is the energy of scattered photon, E is the energy of recoil electron, m_e is the rest mass of an electron, and c is the speed of light.

For unpolarized photons, the Klein-Nishina angular distribution function per steradian of solid angle Ω is

$$\begin{aligned} \frac{d\sigma_c^{KN}}{d\Omega}(\theta) &= r_0^2 \frac{1 + \cos^2\theta}{2} \frac{1}{[1 + h\nu(1 - \cos\theta)]^2} \left\{ 1 + \frac{h\nu^2 (1 - \cos\theta)^2}{(1 + \cos^2\theta)[1 + h\nu(1 - \cos\theta)]} \right\} \\ &= \frac{1}{2} r_0^2 \left(\frac{k}{k_0}\right)^2 \left(\frac{k}{k_0} + \frac{k_0}{k} - \sin^2\theta\right) \qquad (cm^2 sr^{-1} electron^{-1}), \end{aligned} \tag{6}$$

$$k_0 = \frac{h\nu_0}{m_e c^2}, \qquad k = \frac{h\nu}{m_e c^2}$$

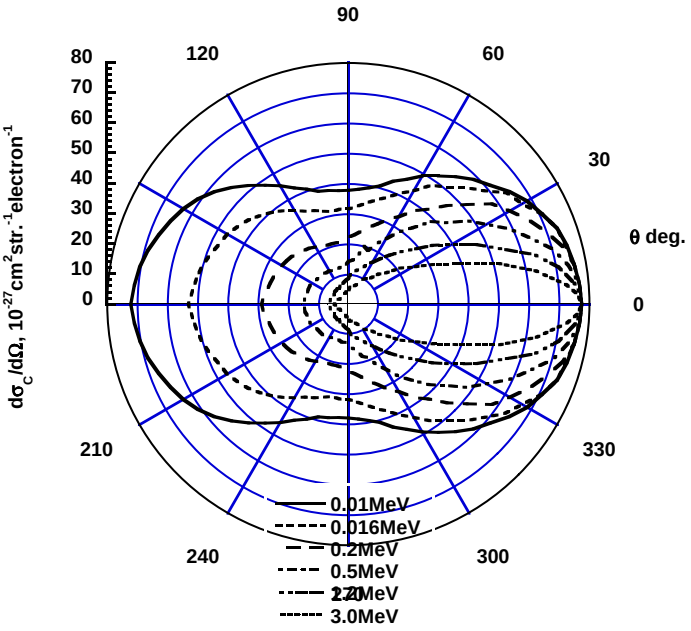

Figure 5: Differential cross section of Compton scattering (original figure from [17]).

where r_0 is the classical electron radius. This angular distribution is shown in Fig. 5.

Integration of Eq. 6 over all angles gives the total Klein-Nishina cross section,

$$\sigma_C^{KN} = 2\pi r_0^2 \left\{ \frac{1+k}{k^2} \left[\frac{2(1+k)}{1+2k} - \frac{\ln(1+2k)}{k} \right] + \frac{\ln(1+2k)}{2k} - \frac{1+3k}{(1+2k)^2} \right\} \quad (cm^2 electron^{-1}). \tag{7}$$

4.1.1 Electron binding correction in Compton scattering

The Klein-Nishina formula for Compton scattering from atomic electrons assume that the electrons are free and at rest, which is a good approximation for photons of the order of 1 MeV or higher, particularly for low-Z target materials.

Binding corrections have usually been treated by the impulse approximation or by Waller-Hatree theory[18], taking account not only of the K-shell, but all of the atomic electrons. This involves applying a multiplicative correction, the so-called "incoherent scattering function", $S(q, X)$, to the differential Klein-Nishina formula,

$$\frac{d\sigma_C^{BD}}{d\Omega}(\theta) = S(q, Z) \frac{d\sigma_C^{KN}(\theta)}{d\Omega}. \tag{8}$$

The momentum transfer, q, is related to the photon energies and deflection angle, θ, according to

$$q = \sqrt{k_0^2 + k^2 - 2k_0 k \cos\theta}, \tag{9}$$

where q is in $m_e c^2$ units and k_0 and k are the photon energies (in $m_e c^2$ units) before and after deflection.

Incoherent scattering functions have been surveyed and studied by Hubbelle *et al.*[3, 4] and are presented for all elements Z=1 to 100, for photon energies 100 eV to 100MeV.

Fig. 6 shows the ratios of σ_C^{BD} to σ_C^{KN} for photon energies of 1, 10, and 100keV

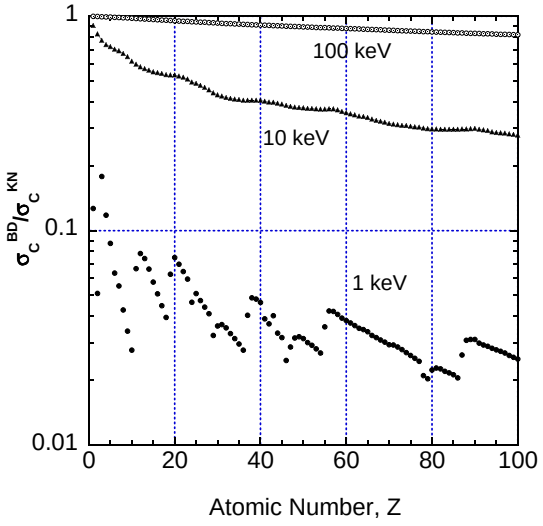

Figure 6: Ratio of the bound-electron Compton scattering cross section, σ_C^{BD}[9], to that for free electrons, σ_C^{KN}, evaluated from the Klein-Nishina formula.

4.1.2 Doppler broadening

In the energy region where the binding correction is necessary, the motion of the atomic electrons around the atomic nucleus gives rise to a Doppler broadening of the apparent energy of the incident photon, resulting in a corresponding broadening of the Compton "modified line" for a given deflection angle of the outgoing scattered photon. The shape of this broadened line is called the "Compton profile." Available data on Compton profiles have been surveyed by Hubbell, and are presented in Ref. [4].

If one is interested in the spectral distribution of Compton-scattered photons, and not just the integrated cross section, Namito *et al.*[19] have made it dramatically clear by computing the scattered spectrum with and without including Doppler broadening in the EGS4 code[20], because such broadening must be included in order to replicate the corresponding measurements using 40 keV photons from a 2.5 GeV synchrotron light source (KEK-PF) (see Fig. 7).

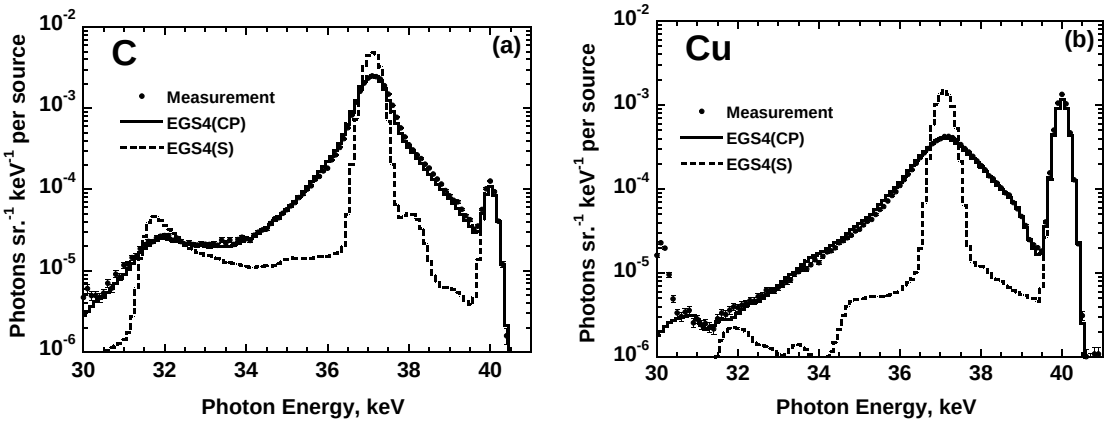

Figure 7: Comparison of the photon spectra scattered by C and Cu samples. The measured and calculated values are shown in symbols and histograms, respectively (k_0=40 keV, $\theta = 90°$). The EGS4 calculation including Doppler broadening is shown as EGS4(CP). The EGS4 calculation without Doppler broadening is shown as EGS4(S). The peak at 30 keV is the Ge K X-ray escape peak of the Rayleigh-scattering peak at 40 keV.

4.2 Rayleigh scattering

Rayleigh scattering is a process by which photons are scattered by bound atomic electrons and in which the atom is neither ionized nor excited. The scattering from different parts of the atomic charge distribution is thus "coherent," i.e., there are interference effects.

This process occurs mostly at low energies and for high-Z material, in the same region where electron binding effects influence the Compton-scattering cross section. In practice, it is necessary to consider the charge distribution of all electrons at once. This can be done approximately through the use of an "atomic form factor", $F(q, Z)$, based on the Thomas-Fermi, Hartree, or other model of the atom. The square of this form factor, $[F(q, Z)]^2$, is the probability that the Z electrons of an atom take up the recoil momentum, q, without absorbing any energy. In this process q is well-represented by the following equation, since it is assumed that $k_0 - k = 0$:

$$q = 2k \sin \frac{\theta}{2}. \tag{10}$$

The differential Rayleigh scattering cross section for unpolarized photons is

$$\frac{\sigma_R}{d\Omega}(\theta) = \frac{r_0^2}{2}(1 + \cos^2 \theta)[F(q, Z)]^2 \ (cm^2 sr^{-1} atom^{-1}). \tag{11}$$

The cumulative angular distributions of σ_R, based on the values of $F(q, Z)$ from Nelms and Oppenheim[21], are displayed in Fig. 8 for C, Fe, and Hg. At high energies it is seen that Rayleigh scattering is conned to a small angle (at 1 MeV more than half the photons are scattered by lee than 5°). At low energies, particularly for high-Z materials, the angular distribution is much broader.

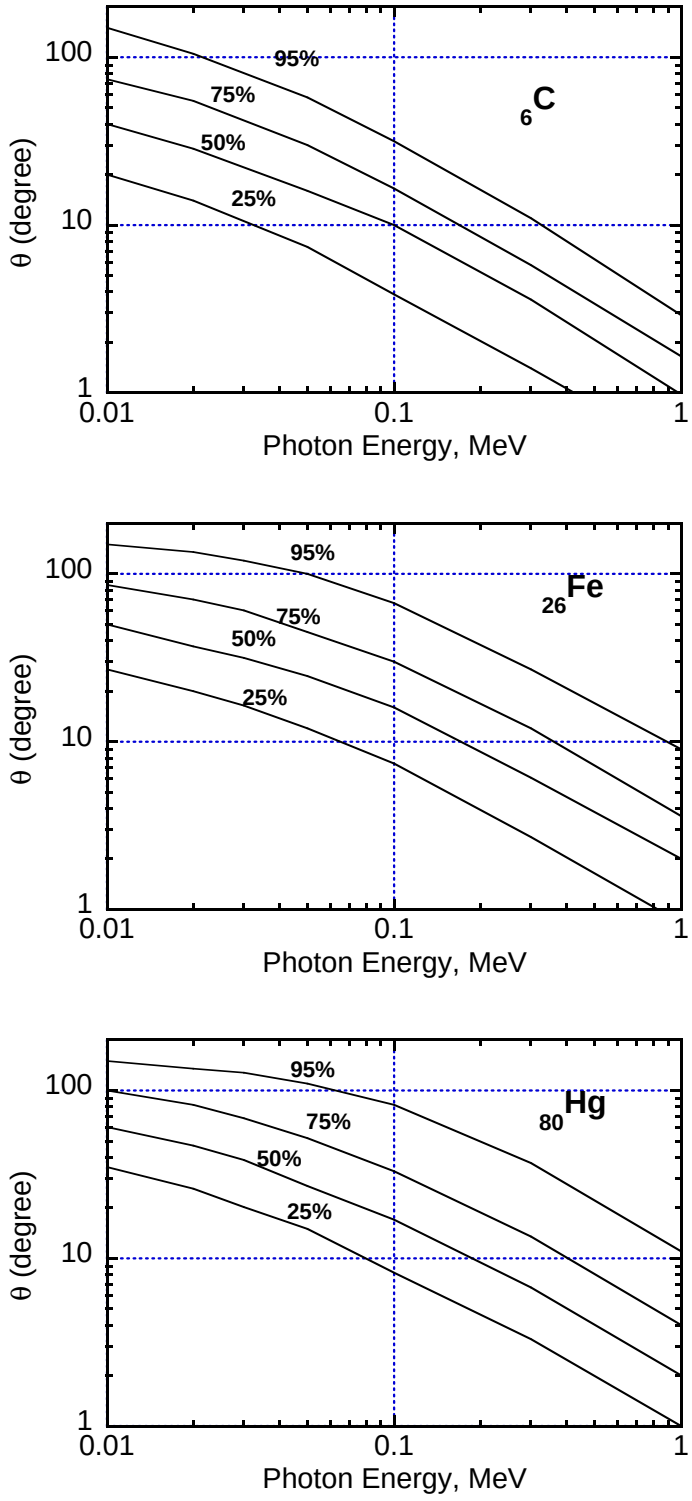

Figure 8: Opening half-angle, θ, of cone containing 25%, 50%, and 95%, respectively, of photons Rayleigh scattered from C, Fe, and Hg.

4.3 Polarization effects

Linear polarization is important in low-energy photon transport, because photons are linearly polarized in scattering; further, the Compton and Rayleigh scattering of linearly polarized photons are anisotropic in their azimuthal distributions in the low-energy region.

For linearly polarized photons with a free electron, the Klein-Nishina angular distribution function per steradian of solid angle Ω is[16]

$$\frac{d\sigma_C^{KN}}{d\Omega} = \frac{1}{4} r_0^2 \left(\frac{k}{k_0}\right)^2 \left(\frac{k}{k_0} + \frac{k_0}{k} - 2 + 4\cos^2\Theta\right). \tag{12}$$

Here, Θ is the angle between the incident polarization vector ($\vec{e}_0$) and the scattered polarization vector ($\vec{e}$). According to Heitler[22], two directions are considered for $\vec{e}$, *i.e.* $\vec{e}$ either in the same plane as $\vec{e}_0$ ($\vec{e}_{||}$) or perpendicular to $\vec{e}_0$ ($\vec{e}_{\perp}$).

The elastic scattering of a photon by one electron is called Thomson scattering. The Thomson-scattering cross section per electron for a linearly polarized photon is[23]

$$\frac{d\sigma_T}{d\Omega} = r_0^2 \cos^2\Theta. \tag{13}$$

Linearly polarized photon scattering for both Compton- and Rayleigh-scattering have been implemented to the EGS4 code by Namito *et al*[24]. The effect of linear polarization is clearly presented in Fig. 9[25], which gives a comparison between EGS4 calculations with and without including linear polarization and Doppler broadening and corresponding measurements using 40 keV linearly polarized photons from a KEK-PF.

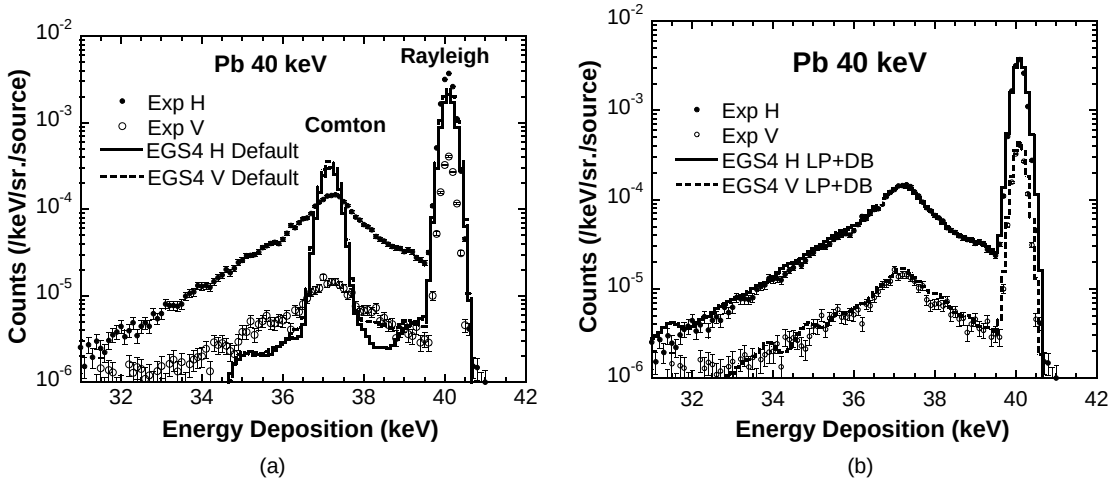

Figure 9: Comparison of the photon spectra scattered by a Pb sample. Source photons are linearly polarized in the vertical direction. The measured and calculated values are indicated by symbols and histograms, respectively (k_0=40 keV, $\theta = 90°$). (a) is the comparison with the EGS4 calculation without including linear polarization and Doppler broadening and (b) is the one with linear polarization and Doppler broadening.

5 Electron-Positron Pair Production

In this effect, which is the most likely photon interaction at high energies, a photon disappears in the field of a charged particle, and an electron-positron pair appears.

For the reaction $M_1 + M_2 \longrightarrow M_3 + M_4 + M_5 + Q$, it can be shown from the conservation of energy and momentum that the threshold energy for the reaction in laboratory system is

$$T_{th}^{lab} = \frac{Q}{2M_2c^2}[Q - 2(M_1c^2 + M_1c^2)] \tag{14}$$

when M_2 is at rest. In a pair-production reaction ($\gamma + M \longrightarrow M + m_e + m_e + Q$),

$$\begin{aligned} M_1 &= 0, \\ M_2 &= M_3 = M, \\ M_4 &= M_5 = m_e, \end{aligned}$$

so that

$$Q = -2m_ec^2(-T_{th}^{CM}) \tag{15}$$

and

$$T_{thh}^{lab} = \frac{2m_ec^2(m_2c^2 + Mc^2)}{Mc^2}. \tag{16}$$

Thus;

1. Pair production in the field of a nucleus of mass M ($M \gg m_e$):

$$T_{th}^{lab} \simeq \frac{2m_ec^2}{Mc^2}(Mc^2) = 2m_ec^2 = 1.022 \text{)MeV}) \tag{17}$$

2. Pair production in the field of an electron ($M = m_e$):

$$T_{th}^{lab} = \frac{2m_ec^2}{m_ec^2}(m_ec^2 + m_ec^2) = 4m_ec^2 = 2.044 \text{)MeV}) \tag{18}$$

The cross section σ_n for pair production in the field of a nucleus varies as

$$\sigma_n \sim Z^2. \tag{19}$$

For low photon energies,

$$\kappa_n (= \frac{N_A}{uA}\sigma_n) \sim \ln(h\nu). \tag{20}$$

For high energies[26],

$$\kappa_n \sim \frac{7}{9X_0}, \tag{21}$$

where X_0 is the radiation length of the material. The quality of the approximation is shown in Table 2 (κ_n for 1000 MeV).

Table 2. Pair-production cross section in the field of a nucleus[27].

Material	$X_0(g\ cm^{-2})$	$\frac{7}{9X_0}(cm^2\ g^{-1})$	$\kappa_n(cm^2\ g^{-1})$	% Difference
Pb	6.40	0.122	0.114	7
Cu	13,0	0.060	0.055	9
Fe	13.9	0.056	0.051	10
Al	24.3	0.032	0.028	14
C	43.3	0.018	0.014	29
H_2O	36.4	0.021	0.020	5

The energy distribution of an electron and positron pair for Pb is shown in Fig. 10[22].

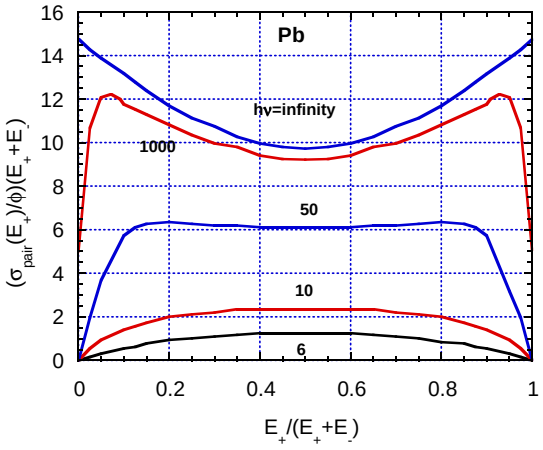

Figure 10: Energy distribution of an electron-positron pair for Pb. E_+ and E_- are the kinetic energy of a positron and an electron, respectively. $\sigma_{pair}(E_+)dE_+$ means the differential cross section which produces a positron between E_+ and $E_+ + dE_+$. $\phi = Z^2 r_e^2/137$.

The cross section, σ_{trip} (triplet), in the field of one of the atomic electrons varies as Z times the square of the unit charge, or

$$\sigma_{trip} \sim Z, \tag{22}$$

and is of minor importance, except for the lowest-Z materials.

This cross section is usually called the "triplet" cross section, since the atomic electron involved in this process is also ejected from the atom, giving rise to trident signature, including the created electron and positron, when observed in a cloud chamber.

Finally, the "characteristic" angle between the direction of motion of the photon and one (or the other) of the electrons ($\pm$) is given by

$$\theta \sim \frac{m_e c^2}{h\nu}\ \text{(inradian)}. \tag{23}$$

6 Mass Attenuation Coefficient and Energy-Absorption Coefficients

6.1 Mass attenuation coefficient, μ/ρ

A narrow beam of monoenergetic photons with an incident intensity I_0, penetrating a layer of material with mass thickness x and density ρ, emerges with intensity I, given by the exponential attenuation law,

$$I/I_0 = \exp[-(\mu/\rho)x]. \tag{24}$$

This equation can be rewritten as

$$\mu/\rho = x^{-1} \ln(I_0/I), \tag{25}$$

from which μ/ρ can be obtained from measured values of I_0, I and x. The various experimental arrangements and techniques from which μ/ρ can be obtained, particularly in the crystallographic photon energy/wavelength regime, have been examined and assessed by Creagh and Hubbell[29, 30] as part of the International Union of Crystallography (IUCr) X-Ray Attenuation Project.

The theoretical value of μ/ρ is defined with the total cross section per atom, σ_{tot}, which is related to μ/ρ according to

$$\mu/\rho = \sigma_{tot} \frac{N_A}{uA}. \tag{26}$$

In this equation, N_A is Avogadro's number (6.022045×10^{23} mol^{-1}), u is the atomic mass unit (1/12 of the mass of an atom of nuclide ^{12}C), A is the relative atomic mass of the target element. Total cross section can be written as the sum over contributions from the principal photon interactions,

$$\sigma_{tot} = \sigma_{pe} + \sigma_{coh} + \sigma_{incoh} + \sigma_{pair} + \sigma_{trip} + \sigma_{ph.n}. \tag{27}$$

Photonuclear absorption can contributed as much as 5-10% to the total photon interaction cross section in a fairly narrow energy region, usually occurring somewhere between 5 and 40 MeV. This cross section has not been included in the theoretical tabulations of the total cross section because of the difficulties due to (a) the irregular dependence of both the magnitude and resonance-shape of the cross section as a function of both Z and A; (b) the gaps in the available information, much of which is for separated isotopes or targets otherwise differing from natural isotope mixtures; and (c) the lack of theoretical models for $\sigma_{ph.n.}$ comparable to those available for calculations of the other cross sections of interest.

μ/ρ without including photonuclear absorption is calculated according to

$$\mu/\rho = \frac{N_A}{uA}(\sigma_{pe} + \sigma_{coh} + \sigma_{incoh} + \sigma_{pair} + \sigma_{trip}). \tag{28}$$

6.2 Mass energy-absorption coefficient, μ_{en}/ρ

The mass energy-absorption coefficients, μ_{en}/ρ (cm^2/g or m^2/kg, ρ is a density of the medium), is a useful parameter in computations of energy deposited in media subjected to photon irradiation. μ_{en}/ρ can be described more clearly through the use of an intermediate quantity, the mass energy-transfer coefficient, μ_{tr}/ρ.

The mass energy-transfer coefficients, μ_{tr}/ρ, when multiplied by the photon energy fluence Ψ ($\Psi = \Phi h\nu$, where Φ is the photon fluence and $h\nu$ is the photon energy), gives the dosimetric

quantity *kerma*. Kerma has been defined[28] as the sum of the kinetic energies of all those primary charged particles released by uncharged particles (here photons) per unit mass. Thus, μ_{tr}/ρ takes into account the escape of secondary photon radiations produced at the initial photon-atom interaction site, plus, by convention, the quanta of radiation from the annihilation of positrons (assumed to have come to rest) originating in the initial pair-production interactions.

Hence, μ_{tr}/ρ is defined as

$$\mu_{tr}/\rho = \frac{N_A}{uA}(f_{pe}\sigma_{pe} + f_{inco}\sigma_{incoh} + f_{pair}\sigma_{pair} + f_{trip}\sigma_{trip}). \tag{29}$$

In this expression, coherent scattering has been omitted because of the negligible energy transfer associated with it, and the factor f represents the average fraction of the photon energy, $h\nu_0$, that is transferred to kinetic energy of charged particles in the remaining types of interactions. These energy-transfer fractions are given by

$$f_{pe} = 1 - (X/h\nu_0), \tag{30}$$

where X is the average energy of fluorescence radiation emitted per absorbed photon,

$$f_{incoh} = 1 - (< h\nu > + X)/h\nu_0, \tag{31}$$

where $< h\nu >$ is the average energy of the Compton-scattered photon.

Also,

$$f_{pair} = 1 - 2m_e c^2/h\nu_0 \tag{32}$$

and

$$f_{trip} = 1 - (2m_e c^2 + X)/h\nu_0. \tag{33}$$

The mass energy-absorption coefficient involves further emission of radiation produced by charged particles in traveling through the medium, and is defined as

$$\mu_{en}/\rho = (1 - g)\mu_{tr}/\rho. \tag{34}$$

The factor g represents the average fraction of the kinetic energy of secondary charged particles (produced in all the type of interactions) that is subsequently lost in radiative energy-loss processes as the particles slow to rest in the medium. The evaluation of g is accomplished by integrating the cross section for the radiative process of interest over the differential track-length distribution established by the particles in the course of slowing down.

Various calculations and compilations were performed for μ_{en}/ρ. Most recent results were presented by Hubbell and Seltzer[6]. Fig. 11 shows a comparison between μ/ρ and μ_{en}/ρ for lead presented in their paper.

The mass energy-absorption coefficients when multiplied by the photon energy fluence, Ψ, gives the absorbed dose of the materials if charged-particle equilibrium exists. The mass energy-absorption coefficients are used in cavity-chamber theory together with the mass stopping power.

7 Photon Cross Section Data Base

Data on the scattering and absorbing of photons, which are explained in previous sections, are required for many scientific, engineering and medical applications. Available tables[1, 6, 31, 32, 33, 34, 35, 36, 37, 38, 39, 40, 41, 42, 43] usually include cross sections for many (but not all) elements. Some tables[1, 31, 35, 40] also contain data for a limited number of compounds and mixtures.

It is possible to generate the cross sections and attenuation coefficients fir any element, compound or mixtures at energies between 1 keV and 100 GeV with a computer program called XCOM[45]. A PHOTX[9] data base was prepared using this XCOM.

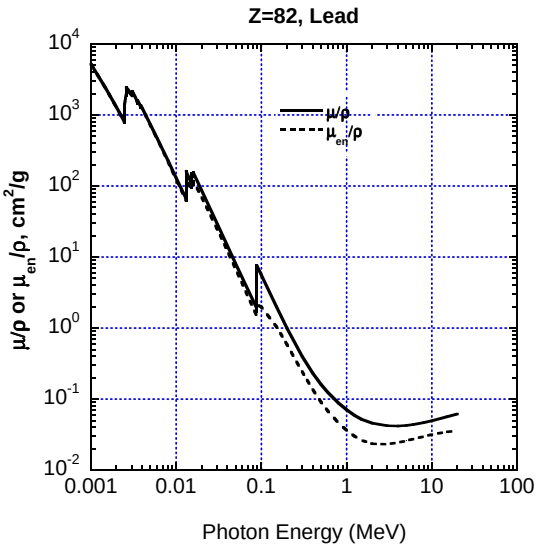

Figure 11: Mass attenuation coefficient, μ/ρ, and the mass energy-absorption coefficient, μ_{en}/ρ, as a function of the photon energy for lead.

References

[1] J. H. Hubbell, "Photon Cross Sections, Attenuation Coefficients, and Energy Absorption Coefficients From 10 keV to 100 GeV", *NSDRS-NBS 29*.

[2] J. H. Hubbell, W. J. Veigele,, E. A. Briggs, R. T. Brown, D. T. Cromer, and R. .J. Howerton, "Atomic Form Factors, Incoherent Scattering Functions, and Photon Scattering Cross Sections", *J. Phys. Chem. Ref. Data* **4**(1975)471-616.

[3] J. H. Hubbell, "Polarization Effects in Coherent and Incoherent Photon Scattering: Survey of Measurements and Theory Relevant to Radiation Transport Calculations", *NISTIR 4881*, 1992.

[4] J. H. Hubbell, "Bibliography and Current Status of K, L, and higher Shell Fluorescence Yields for Computations of Photon Energy-Absorption Coefficients", *NISTIR 89-4144*(1994).

[5] J. H. Hubbell, "Tables of X-ray Mass Attenuation Coefficients and Mass Energy-Absorption Coefficients 1 keV to 20 MeV for Elements Z=1 to 92 and 48 Additional Substances of Dosimetric Interest," *NISTIR 5632*, 1995.

[6] J. H. Hubbell, "An Examination and Assessment of Available Incoherent Scattering S-Matrix Theory, also Compton Profile Information, and Their Impact on Photon Attenuation Coefficient Compilations," *NISTIR 6358*, 1999.

[7] U. Fano, L. V. Spencer, M. J. Berger, in Flügge (Ed.), Encyclopedia of Physics, Vol. XXXVIII/2 Berlin/Göttingen/Heidelberg: Springer 1959.

[8] E. Frytag, "Strahlenschutz an hochenergiebschleunigern", (G. Braum, Karlsruhe, 1072).

[9] Radiation Shielding Information Center Data Library Package DLC-136/PHOTX, "Photon Interaction Cross Section Library", contributed by the National Institute of Standards and Technology.

[10] R. W. Fink, R. C. Jopson, H. Mark, and D. C. Swift, "Atomic Fluorescence Yields", *Rev. Mod. Phys* **38**(1966)513-540.

[11] W. Bambynek, B. Crasemann, R. W. Fink, H. -U. Freund, H. Mark, C. D. Swift, R. E. Price, and P. V. Rao, "X-Ray Fluorescence Yields, Auger, and Coster-Kronig Transition Probability", *Rev. Mod. Phys.* **44**(1972)716-813; erratum in bf 46(1974)853.

[12] M. O. Krause, "Atomic Radiative and Radiationles Yields for K and L shells", *Phys. and Chem. Ref. Data* **8** (1979)307-327.

[13] B. Richard, B. Firestone and S. S. Virginia edited, "Table of Isotopes Eighth Edition", John Wiley & Sons, Inc.,1996.

[14] J. H. Scofield, "Relativistic Hartree-Slater Values for K and L X-Ray Emission Rates", *Atomic Data and Nuclear Data Tables* **14**(1974)121-137.

[15] S. L. Salem, S. L. Panossian, and R. A. Krause, "Experimental K and L Relative X-Ray Emission Rate", *Atomic Data and Nuclear Data Tables* **14**(1974)91-109.

[16] O. Klein and Y. Nishina, *Z. Physik* **52** (1929)853-868.

[17] R. D. Evans,"Compton Effect", in Handbuch der Physik XXXIV, Tlügge ed., pp2180298, Springer-Verlag, Berlin (1958).

[18] I. Waller and D. R. Hartree, "On the intensity of total scattering of X-rays", *Proc. R. Soc, London, Ser.* **A 124** (1929)119-142.

[19] Y. Namito, S. Ban and H. Hirayama, "Implementation of the Doppler broadening of a Compton-scattered photon into the EGS4 code", *Nucl. Instr. Meth.* **A349**(1994)489-494.

[20] W. R. Nelson, H. Hirayama and D. W. O. Rogers, "The EGS4 Code System", *SLAC-265*, (1985).

[21] A. T. Nelms and L. J. Oppenheim, *Rev. Nat. Bur. Stds.* **55**(1955)53-62.

[22] W. Heitler, "The Quantum Theory of Radiation", Oxford Univ. Press, Oxford, 1954.

[23] P. P. Kane, *Phys. Rev.* **140**(1986)75.

[24] Y. Namito, S. Ban and H. Hirayama, "Implementation of Linearly-polarized photon scattering into the EGS4 code", *Nucl. Instr. Meth.* **A 332**(1993)277-283.

[25] H. Hirayama, S. Ban and Y. Namito, "Current Status of a Low Energy Photon Transport Benchmark", Presented at Shielding Aspects of Accelerators, Targets and Irradiation Facilities (SATIF5), Paris, France, July 17-21, 2000, *KEK Preprint 2000-65*, July 2000.

[26] B. Rossi, "High Energt Particles", Prentice=Hall, Inc., Englewood Cliffs, New Jersey, 1952.

[27] K. R. Kase and W. R. Nelson, "Concepts of Radiation Dosimetry", Pergamon Press.

[28] "Radiation Quantities and Units", *ICRU Report 33*, Bethesda, MD, 1980.

[29] D. C. Creagh and J. H. Hubbell, "Problems Associated with the Measurement of X-Ray Attenuation Coefficients. I. Silicon", Report on the International Union of Crystallography X-Ray Attenuation Project, *Acta Cryst. A* **43**(1987)102-112.

[30] D. C. Creagh and J. H. Hubbell, "Problems Associated with the Measurement of X-Ray Attenuation Coefficients. II. Carbon", Report on the International Union of Crystallography X-Ray Attenuation Project, *Acta Cryst. A* **46**(1990)402-408.

[31] J. H. Hubbell and M. J. Berger, Section 4.1 and 4.2 in R. G. Jaeger (ed.): Engineering Compendium on Radiation Shielding (IAEA, Viena), Vol. 1, Ch. 4, pp. 167-202, Springer, Berlin (1968),

[32] W. H. McMaster, N. K. DEl Grand, J. H. Malett, J. H. Hubbell, "Compilation of X-ray Cross Sections", Lawrence Livermore Lab., *Report UCRL-50174*, (1969).

[33] E. Storm and H. I. Israel, "Photon Cross Sections from 1 keV to 100MeV for Elements Z=1 to Z=100", *Nucl. Data Tables* **A7**(1970)565-681.

[34] W. J. Weigele, "Photon Cross Sections from 0.1 keV to 1 MeV for elements Z=1 to Z=94", *Atomic Data* **5**(1973)51-111.

[35] J. H. Hubbell, "Photon Mass Attenuation and Mass Energy-Absorption Coefficients for H, C, N, O, Ar and Seven Mixtures from 0.1 keV to 20 MeV", *Radiat. Res.* **70**(1977)58-81.

[36] J. Leroux and T. P. Thinh, "Revised Tables of X-ray mass Attenuation Coefficients", Cororation Scientifique Classique, Quebec (1977).

[37] J. H. Hubbell, H. A. Gimm, and I. Overbo, "Pair, Triplet and Total Atomic Cross Sections (and Mass Attenuation Coefficients) for 1 MeV-200 GeV Photons in Elements Z=1 to 100", *J. Phys. Chem. Ref. Data* **9**(1980)1023-1147.

[38] E. F. Plechaty, D. E. Cullen, and R. J. Howerton, "Tables and Graphs of Photon-Interaction Cross Sections from 0.1 keV to 100 MeV Derived from the LLL Evaluated-Nuclear-Data Library", *Report UCRL-50400*, Vol. 6, Rev. 3 (1981).

[39] B. L. Henke, P. Lee, T. J. Tanaka, R. L. Shimabukuro, and B. K. Fujikawa, "Low Energy X-ray Interaction Coefficients: Photoabsorption, Scattering and Reflection", *Atomic Data and Nuclear Data Tables* **27**(1982)1-144.

[40] J. H. Hubbell, "Photon Mass Attenuation and Energy Absorption Coefficients from 1 keV to 20 MeV, *Int. J. Appl. Radiation & Isotopes* **33**(1982)1269-1290.

[41] S. T. Perkins, et al., "Tables and Graphs of Atomic Subshell and Relaxation Data Derived from the LLNL Evaluated Atomic Data Library (EADL), Z=1-100", Lawrence Livermore National Laboratory, Livermore CA, Vol. 30 (1991).

[42] D. E. Cullen, et al., "Tables and Graphs of Photon-Interaction Cross Sections Derived from the LLNL Evaluated Atomic Data Library (EPDL), Z=1-50", Lawrence Livermore National Laboratory, Livermore CA, Vol. 6, Part A, Rev. 4(1991).

[43] D. E. Cullen, et al., "Tables and Graphs of Photon-Interaction Cross Sections Derived from the LLNL Evaluated Atomic Data Library (EPDL), Z=51-100", Lawrence Livermore National Laboratory, Livermore CA, Vol. 6, Part B, Rev. 4(1991).

[44] Radiation Shielding Information Center Data Library Package DLC-179/ENDLIB-94,"LLNL Libraries of Atomic Data, Electron Data, and Photon Data in Evaluated Nuclear Data Library (ENDL) Type Format", Contributed Lawrence Livermore National Laboratory.

[45] M. J. Berger and J. H. Hubbell, "XCOM: Photon Cross Sections on A Personal Computer", *NBSIR 87-3597*, 1987.